Spectral Stiffness Microplane Model for Unidirectional Composites

Sean E. Phenisee
Sung Lin Tien
Marco Salviato
Paper Number: 226

July 1, 2018

ABSTRACT

The use of unidirectional (UD) composites for primary and secondary structures is becoming broader and broader with applications including aeronautics and astronautics, automotive and bioengineering. However, the efficient use of these materials requires the development of proper computational tools for design. Leveraging the spectral stiffness decompostition of the stiffness tensor and a microplane formulation, the present contribution proposes a computational model to capture the main damage and fracturing mechanisms in UD composites. Preliminary simulations of uniaxial tests are compared to experimental data taken from the "World Wide Failure Exercise" to investigate the predictive capability of the model.

INTRODUCTION

Thanks to their excellent specific mechanical performances and the recent developments in manufacturing technologies, the range of engineering applications of composites is continuously expanding. Composites find applications in land, marine and air transportation, in wind and tidal energy production, and blast protection of civil infrastructures and vehicles. In order to exploit their outstanding characteristics, design tools to describe collapse of composite structures capturing the complex fracture mechanics involved are required.

The present contribution proposes a general constitutive model for composites able to simulate the orthotropic stiffness, prepeak nonlinearity, failure envelopes, and also the post-peak softening and fracture. The framework of the microplane model successfully applied for concrete, steel, rocks, soils, and stiff foams is adopted [1–9]. A key feature of the microplane model is that the constitutive laws are formulated in

Sean E. Phenisee, Department of Aeronautics and Astronautics, University of Washington, Guggenheim Hall, Seattle, WA, 98195
Sung Lin Tien, Greenpoint Technologies, 4600 Carillon Point, Kirkland, WA 98033
Marco Salviato, Department of Aeronautics and Astronautics, University of Washington, Guggenheim Hall, Seattle, WA, 98195

terms of the stress and strain vectors acting on planes of any orientation within the material meso-structure, called the microplanes. These planes can be conceived as the tangent planes of a unit sphere surrounding every point in the three-dimensional space. The microplane strain vectors are the projections of the macroscropic strain tensor, whereas the macroscopic stress tensor is related to the microplane stress vectors via the principle of virtual work. The adoption of vectors rather than tensors makes the approach conceptually clearer while the introduction of microplanes allows to inherently embedding the effect of the mesostructure into the formulation. Finally, the Spectral Stiffness Decomposition theorem [10–12] is used to decompose the stiffness matrix and to define energetically orthogonal strain modes at the microplane level. In this way, the anisotropic behavior is automatically described in the microplane formulation.

THEORETICAL FRAMEWORK

Microplane model

Microplanes are the tangent planes that forms a unit sphere around the material meso-structure. Projection of the macroscopic tensor on the microplanes allows to formulate the constitutive laws in any orientation of three-dimensional space for every single point of the material. Using Kelvin notation, the projection can be written as follows:

$$\boldsymbol{\varepsilon}_P = \boldsymbol{P}\boldsymbol{\varepsilon} \tag{1}$$

where $\boldsymbol{\varepsilon}_P = \left[\varepsilon_N \; \varepsilon_M \; \varepsilon_L\right]^T$ consists of the normal component, ε_N and the shear components, ε_M and ε_L.

The projection matrix,

$$\boldsymbol{P} = \begin{bmatrix} N_{11} & N_{22} & N_{33} & \sqrt{2}N_{23} & \sqrt{2}N_{13} & \sqrt{2}N_{12} \\ M_{11} & M_{22} & M_{33} & \sqrt{2}M_{23} & \sqrt{2}M_{13} & \sqrt{2}M_{12} \\ L_{11} & L_{22} & L_{33} & \sqrt{2}L_{23} & \sqrt{2}L_{13} & \sqrt{2}L_{12} \end{bmatrix} \tag{2}$$

has the size of 3×6 that relates the macroscopic strain tensor to the microscopic strain vector as a function of plane orientation. $N_{ij} = n_i n_j$, $M_{ij} = (m_i n_j + m_j n_i)/2$ and $L_{ij} = (l_i n_j + l_j n_i)/2$, where n_i, m_i and l_i represents i-th component of a vector in the local Cartesian coordinate of a generic microplane. Furthermore, each component is expressed as $n_1 = \sin\theta\cos\varphi$, $n_2 = \sin\theta\sin\varphi$, $n_3 = \cos\theta$ while one can choose $m_1 = \cos\theta\cos\varphi$, $m_2 = \cos\theta\sin\varphi$, $m_3 = -\sin\theta$, $l_1 = -\sin\varphi$, $l_2 = \cos\varphi$ and $l_3 = 0$. This guarantees orthogonality to the coordinate vectors. The local Cartesian coordinates and the spherical reference system corresponding to this formulation are shown in Figure 1. Constitutive laws at the microscopic level are used to compute the microplane stress vector, $\boldsymbol{\sigma}_P$. Then, the macroscopic stress tensor can be obtained via the *principle of virtual work*:

$$\boldsymbol{\sigma} = \frac{3}{2\pi}\int_{\Omega} \boldsymbol{P}^T \boldsymbol{\sigma}_P \mathrm{d}\Omega \tag{3}$$

In the equation, Ω is the surface of a unit sphere representing half of the all the microplane orientations.

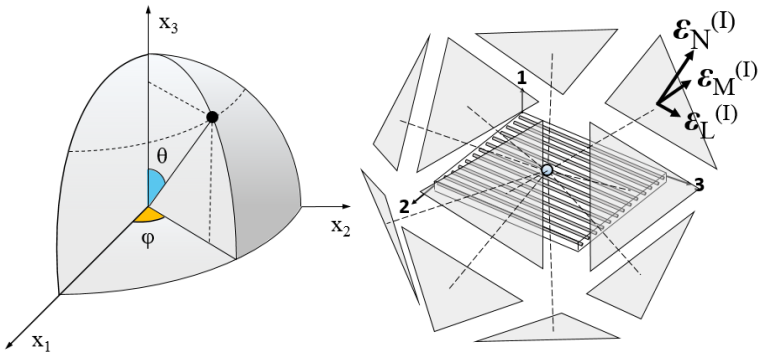

Figure 1. Schematic representation of a UD composite with the associated microplanes and the local spherical coordinate system.

Spectral decomposition of the elastic tensor

In this formulation, stress and strain tensors are decomposed into orthogonal modes using the spectral decomposition theorem. Thanks to Kelvin notation, the constitutive law of a general anisotropic material in the elastic regime is defined as follows:

$$\boldsymbol{\sigma} = \boldsymbol{C}\boldsymbol{\varepsilon} \tag{4}$$

where

$$\begin{aligned} \boldsymbol{\sigma} &= \left[\sigma_{11}\ \sigma_{22}\ \sigma_{33}\ \sqrt{2}\sigma_{23}\ \sqrt{2}\sigma_{13}\ \sqrt{2}\sigma_{12}\right]^T \\ \boldsymbol{\varepsilon} &= \left[\varepsilon_{11}\ \varepsilon_{22}\ \varepsilon_{33}\ \sqrt{2}\varepsilon_{23}\ \sqrt{2}\varepsilon_{13}\ \sqrt{2}\varepsilon_{12}\right]^T \end{aligned} \tag{5}$$

and $\boldsymbol{C}$ is 6×6 stiffness matrix in which each component is computed by the elastic material properties. The factor $\sqrt{2}$ is assigned to the shear components to prevent the inconsistency of the norm between a tensor and a vectorial notation of stress and strain.

In reference to the spectral decomposition theorem, the stiffness matrix can be decomposed corresponding to each eigen-mode:

$$\boldsymbol{C} = \sum_I \lambda^{(I)} \boldsymbol{C}^{(I)} \tag{6}$$

where the eigenvalue of each mode is referred to the superscript, $I = 1, 2...6$ in the equation. $\boldsymbol{C}^{(I)} = \sum_n \boldsymbol{\phi}_{In}\boldsymbol{\phi}_{In}^T$ is the eigenmatrix of corresponding to its eigenvalue and computed by its normalized eigenvector, $\boldsymbol{\phi}_I^T \boldsymbol{C} \boldsymbol{\phi}_I = \lambda^{(I)}$. The number of distinct eigenvalues are closely associated with the number of independent material properties, which depends on the degree of anisotropy.

There are three important properties on the eigenmatrices, $\boldsymbol{C}^{(I)}$:

1. *partition of unity*, $\sum_I \boldsymbol{C}^{(I)} = \boldsymbol{I}$;

2. *orthogonality*, $\boldsymbol{C}^{(I)}\boldsymbol{C}^{(J)} = 0$ when $I \neq J$;

3. *idempotent*, $\boldsymbol{C}^{(I)}\boldsymbol{C}^{(I)} = \boldsymbol{C}^{(I)}$.

The eigenmatricies are used to compute the eigenstresses and eigenstrains which represent the decomposed stress and strain tensors in the energetically orthogonal modes, meaning that $\delta\mathcal{W}_{IJ} = \boldsymbol{\sigma}_I^T \delta\boldsymbol{\varepsilon}_J = \lambda^{(I)}\boldsymbol{\varepsilon}_I^T \delta\boldsymbol{\varepsilon}_J = \lambda^{(I)}\boldsymbol{\varepsilon}^T \mathbf{C}^{(I)}\mathbf{C}^{(J)}\delta\boldsymbol{\varepsilon} = 0$. They are expressed as follows:

$$\boldsymbol{\sigma}_I = \boldsymbol{C}^{(I)}\boldsymbol{\sigma} \quad \text{and} \quad \boldsymbol{\varepsilon}_I = \boldsymbol{C}^{(I)}\boldsymbol{\varepsilon} \tag{7}$$

It is worth mentioning that $\boldsymbol{\sigma} = \sum_I \boldsymbol{\sigma}_I$ and $\boldsymbol{\varepsilon} = \sum_I \boldsymbol{\varepsilon}_I$.

Knowing that the compliance matrix is inverse of the stiffness matrix, $\mathbf{S} = \mathbf{C}^{-1}$, it can be shown that:

$$\boldsymbol{S} = \sum_I \left(\lambda^{(I)}\right)^{-1} \boldsymbol{S}^{(I)} \tag{8}$$

Which implies that eigenmatrices of compliance matrix is equal to that of stiffness matrix, $\mathbf{S}^{(I)} = \mathbf{C}^{(I)}$.

Microplane model with spectral decomposition

In this microplane model, the spectral decomposition of strain and stress tensors was used to address the material anisotropy [1–3, 10–12]. The projection of each orthogonal eigenstrain tensor can represent each microplane vectors into microplane eigenstrain vectors as follows:

$$\boldsymbol{\varepsilon}_P = \sum_I^N \boldsymbol{\varepsilon}_P^{(I)} \qquad \text{where} \begin{cases} \boldsymbol{\varepsilon}_P^{(I)} = \boldsymbol{P}\boldsymbol{\varepsilon}^{(I)} = \boldsymbol{P}^{(I)}\boldsymbol{\varepsilon} \\ \boldsymbol{P}^{(I)} = \boldsymbol{P}\boldsymbol{C}^{(I)} \end{cases} \tag{9}$$

where N is the number of independent eigenvalues.

Application to unidirectional composites

A cartesian coordinate system to represent a unidirectional composite is defined such that *1* is aligned with the thickness direction, *2* is aligned with in-plane matrix direction and *3* is aligned with the fiber direction. This coordinate system is shown in Figure 1. Planes *1-2*, *2-3* and *1-3* are the planes of material symmetry, indicating that the material is orthotropic. Moreover, it is also worth notice that the plane *1-2* is plane of isotropy, so the out-of-plane shear property is closely related to the properties of matrix. As a result of existence of plane of isotropy, the number of independent elastic properties reduces to 5. Hence, the elastic compliance matrix, S, can be expressed as follows:

$$\boldsymbol{S} = \begin{bmatrix} 1/E & -\nu/E & -\nu'/E & 0 & 0 & 0 \\ -\nu/E & 1/E & -\nu'/E & 0 & 0 & 0 \\ -\nu'/E & -\nu'/E & 1/E' & 0 & 0 & 0 \\ 0 & 0 & 0 & 1/2G' & 0 & 0 \\ 0 & 0 & 0 & 0 & 1/2G' & 0 \\ 0 & 0 & 0 & 0 & 0 & 1/2G \end{bmatrix} \tag{10}$$

where $E = E_1 = E_2$, $E^{'} = E_3$, $\nu = \nu_{12} = \nu_{21}$, $\nu^{'} = \nu_{13} = \nu_{23}$, and $G^{'} = G_{13} = G_{23}$. The elastic stiffness matrix can be computed by taking inverse of the elastic compliance matrix.

The eigenvalues of the elastic stiffness matrix are:

$$\begin{aligned}
\left(\lambda^{(1)}\right)^{-1} &= \frac{1+\nu}{E} \\
\left(\lambda^{(2)}\right)^{-1} &= \frac{1}{2E'} + \frac{1-\nu}{2E} - \sqrt{\left(\frac{1-\nu}{2E} - \frac{1}{2E'}\right)^2 + 2\left(\frac{\nu'}{E}\right)^2} \\
\left(\lambda^{(3)}\right)^{-1} &= \frac{1}{2E'} + \frac{1-\nu}{2E} + \sqrt{\left(\frac{1-\nu}{2E} - \frac{1}{2E'}\right)^2 + 2\left(\frac{\nu'}{E}\right)^2} \\
\left(\lambda^{(4)}\right)^{-1} &= \frac{1}{2G} = \frac{1+\nu}{E} \\
\left(\lambda^{(5)}\right)^{-1} &= \frac{1}{2G'}
\end{aligned} \tag{11}$$

The related eigematrices, constructed from the normalized eigenvectors, are:

$$\begin{aligned}
C_{ij}^{(1)} &= \frac{(\delta_{i1} - \delta_{i2})(\delta_{1j} - \delta_{2j})}{2} \\
C_{ij}^{(2)} &= \frac{0.5\chi^2\left(\delta_{i1} + \delta_{i2} - \delta_{3j} + \delta_{i3}\delta_{3j}\right) + \chi\left(\delta_{i3} + \delta_{3j} - 2\delta_{i3}\delta_{3j}\right) + 2\left(\delta_{i3}\delta_{3j}\right)}{2 + \chi^2} \\
C_{ij}^{(3)} &= \frac{0.5\xi^2\left(\delta_{i1} + \delta_{i2} - \delta_{3j} + \delta_{i3}\delta_{3j}\right) + \xi\left(\delta_{i3} + \delta_{3j} - 2\delta_{i3}\delta_{3j}\right) + 2\left(\delta_{i3}\delta_{3j}\right)}{2 + \xi^2} \\
C_{ij}^{(4)} &= \delta_{i6}\delta_{6j} \\
C_{ij}^{(5)} &= \delta_{i5}\delta_{5j} + \delta_{i4}\delta_{4j}
\end{aligned} \tag{12}$$

where δ_{ij} is Kronecker delta, $i, j = 1, 2...6$ and χ and ξ are dimensionless constants:

$$\begin{aligned}
\chi &= \frac{E - E^{'}(1-\nu)}{2E'\nu'} + \sqrt{\left[\frac{E - E'(1-\nu)}{2E'\nu'}\right]^2 + 2} \\
\xi &= \frac{E - E^{'}(1-\nu)}{2E'\nu'} - \sqrt{\left[\frac{E - E'(1-\nu)}{2E'\nu'}\right]^2 + 2}
\end{aligned} \tag{13}$$

After computing eigenvalues and eigenmatricies, the normal, $\varepsilon_N^{(I)}$, and total shear $\varepsilon_T^{(I)} = \sqrt{\left(\varepsilon_M^{(I)}\right)^2 + \left(\varepsilon_L^{(I)}\right)^2}$ components of the microplane strain vector can be obtained by the projection. As is evident, each component depends on the orientation of each microplane, the material properties and the macroscopic strains.

Distribution of the normal component of microplane strain vectors

The normal component of the microplane strain vector is used to identify whether the plane is under a tension or compression. Shear modes (mode 4 and 5) are completely isolated from the rest of modes when there is no shear strain in macroscopic

sense. Since only mode 1, 2 and 3 get activated when the macroscopic loading does not include a shear component, the effective normal strain introduced to account for the overall deformation of the material only contains these three modes and defined as follows:

$$\varepsilon_N^{eff} = \frac{\lambda_1}{\lambda_2}\varepsilon_N^{(1)} + \varepsilon_N^{(2)} + \frac{\lambda_3}{\lambda_2}\varepsilon_N^{(3)} \tag{14}$$

If the effective normal strain is less than zero, the corresponding microplane is assumed to be under compression; otherwise, assumed to be under tension. A distribution of $\varepsilon_N^{(I)}$ in each mode provides an overall deformation of the microplane sphere in each mode under the specific loading condition. Understanding these modal responses provides an insight constructing the interaction among the mode 1, 2 and 3, which leads to define correct failure conditions of the material.

It was desired to assign physical interpretations to each mode or combination of modes as in Salviato et al. [3]. However, there are only clear isolation between the normal modes (mode 1, 2 and 3) and the shear modes (mode 4 and 5). To characterize the behavior/deformation/response of the material under tensile or compressive loading, all three modes have to be considered instead of treating each mode separately in calibration. However, each mode can still be associated with the specific material behavior based on the dominant response to the loading direction. As an example, mode 1 gets activated only when there is a break of the symmetry in deformation of plane of isotropy. Therefore, mode 1 normal strain, $\varepsilon_N^{(1)}$ is zero when loading is perpendicular to fiber axis (axis-3). From this result, mode 1 was chosen to be the dominant mode calibrating the matrix properties. In contrast, mode 2 and 3 equally contribute when the symmetry in the plane of isotropy is conserved. Therefore, mode 2 and 3 were chosen to be the dominant modes calibrating the fiber properties.

Constitutive law in the elastic regime

Constitutive behavior in the elastic regime can be assumed similar to the Hooke's law. This assumption states that the normal and shear eigenstresses on the microplanes are proportional to the corresponding eigenstrain.

$$\sigma_N^{(I)} = \lambda^{(I)}\varepsilon_N^{(I)}, \quad \sigma_M^{(I)} = \lambda^{(I)}\varepsilon_M^{(I)}, \quad \sigma_L^{(I)} = \lambda^{(I)}\varepsilon_L^{(I)} \tag{15}$$

where $\lambda^{(I)} =$ refers to the I-th eigenvalues. It is important to keep in mind that this relation is only relevant in elastic regime. Once the material undergoes damaging this relation is not valid.

Failure criteria for tensile and compressive loading conditions

In order to capture different types of failure mechanisms, it is important to identify the orientation of the critical microplane that will go under softening first and lead to the damage initiation. From the study on the distribution of the normal component of microplane strain vector, ε_N, Mode 1, 2 and 3 get activated on tensile or compressive loading, meaning that the failure criteria should involve these three modes. Furthermore, the close association of mode 1 to matrix response lead to the selection of mode 1 to be the dominant factor deciding the failure in matrix. Other two modes

which have closer relation with the loading along the fiber direction are coupled to describe fiber failures. Mode 23 is defied such that:

$$\varepsilon_N^{(23)} = \frac{\lambda_3}{\lambda_2}\varepsilon_N^{(3)} + \varepsilon_N^{(2)}, \quad \varepsilon_M^{(23)} = \frac{\lambda_3}{\lambda_2}\varepsilon_M^{(3)} + \varepsilon_M^{(2)}, \quad \varepsilon_L^{(23)} = \frac{\lambda_3}{\lambda_2}\varepsilon_L^{(3)} + \varepsilon_L^{(2)} \tag{16}$$

Again, Total shear strain is defined as $\varepsilon_T^{(23)} = \sqrt{\left(\varepsilon_M^{(23)}\right)^2 + \left(\varepsilon_L^{(23)}\right)^2}$.

A quadratic criterion was assumed for the mixed mode tensile cracking. Tensile failure criterion is defined as follows:

$$1 = \left(\frac{\sqrt{\varepsilon_{N_1}^2 + \varepsilon_{T_1}^2}}{\chi_1}\right)^2 + \left(\frac{\sqrt{\varepsilon_{N_{23}}^2 + \varepsilon_{T_{23}}^2}}{\chi_{23}}\right)^2 \tag{17}$$

χ_1 and χ_{23} are the calibration parameters associated with the tensile strength in transverse direction and longitudinal direction of UD composite, respectively.

Similarly, a quadratic criterion was assumed for the mixed mode compressive cracking. However, there are two additional parameters introduced: β_1 and β_{23} which are closely related to the angle of the crack propagation under a compressive loading. Compressive failure criterion is defined as follows:

$$1 = \left(\frac{\sqrt{(\beta_1\varepsilon_{N_1})^2 + \varepsilon_{T_1}^2}}{\gamma_1}\right)^2 + \left(\frac{\sqrt{(\beta_{23}\varepsilon_{N_{23}})^2 + \varepsilon_{T_{23}}^2}}{\gamma_{23}}\right)^2 \tag{18}$$

γ_1 and γ_{23} are the calibration parameters associated with the compressive strength in transverse direction and longitudinal direction of UD composite, respectively.

Unlike tensile cracking, the band of damaged region from the compressive loading is not perpendicular to the loading direction due to shear dominated cracking. When the compression is in transverse direction, matrix carry the most of the load, and the dominant failure mechanism is shear crack in matrix. The critical microplane, leading this type of failure, should be shear dominated with the friction from the normal stress component. The orientation of this plane can be identified by calibrating β_1.

When the compression is in longitudinal direction, fibers carry the most of the loading, and the formulation of fiber kink band is the dominant failure mechanism. Imperfection in fiber alignment from manufacturing process causes the local shear stress near the misaligned fibers. As the compressive loading increases, not only the shear stiffness of matrix degrade but also induces localized fiber bending, which raise the local shear stress, worsen th resistance in shear, and increase the rotation angle. Once the shear stress near the localized region of fiber banding reaches the critical value, matrix cannot resist the further rotation, and the kink band forms. The critical microplane representing imperfect fibers should have non-zero components but the normal strain should still be dominant since the misalignment angle is not usually not large. The orientation o the critical plane can be identified by calibrating β_{23}.

Constitutive law in the inelastic regime

According to Cusatis et al. [13,14], a microplane effective eigenstrain for a generic *I*-th eigenmode is defined as follows:

$$\varepsilon^{(I)} = \sqrt{\left(\varepsilon_N^{(I)}\right)^2 + \left(\varepsilon_T^{(I)}\right)^2} \tag{19}$$

The relation between the stress and strain in microplanes can be obtained by imposing the consistency of virtual work:

$$\begin{aligned} \delta\mathcal{W}_I = \sigma^{(I)}\delta\varepsilon^{(I)} &= \frac{\sigma^{(I)}}{\varepsilon^{(I)}}\left(\varepsilon_N\delta\varepsilon_N + \varepsilon_M\delta\varepsilon_M + \varepsilon_L\delta\varepsilon_L\right)^{(I)} \\ &= \left(\sigma_N\delta\varepsilon_N\right)^{(I)} + \left(\sigma_M\delta\varepsilon_M\right)^{(I)} + \left(\sigma_L\delta\varepsilon_L\right)^{(I)} \end{aligned} \tag{20}$$

The energy dissipated on each microplane should be non-negative in order to satisfy a sufficient condition for the second law of thermodynamics. Thanks to the definition in Eq. 19 and to Eq. 20, $\delta\mathcal{W}_I \geq 0$ for all the microplanes. As a consequence of Eq. 20, the relations between the normal and shear stresses and the corresponding normal and shear strains can be expressed:

$$\sigma_N^{(I)} = \left(\sigma\frac{\varepsilon_N}{\varepsilon}\right)^{(I)}, \quad \sigma_M^{(I)} = \left(\sigma\frac{\varepsilon_M}{\varepsilon}\right)^{(I)}, \quad \sigma_L^{(I)} = \left(\sigma\frac{\varepsilon_L}{\varepsilon}\right)^{(I)} \tag{21}$$

The *I*-th effective stress are defined similar to the *I*-th effective strain:

$$\sigma^{(I)} = \sqrt{(\sigma_N^{(I)})^2 + (\sigma_T^{(I)})^2} \quad \text{where } \sigma_T^{(I)} = \sqrt{(\sigma_M^{(I)})^2 + (\sigma_L^{(I)})^2} \tag{22}$$

The effective stress is assumed to be incrementally elastic.

INELASTIC BEHAVIOR UNDER TENSILE/COMPRESSIVE LOADING

Motivated from the definition of the effective strain, other measure of the strain called the equivalent strain is introduced to construct the convenient inelastic relation in the microplane. Equivalent strain for the tensile loading is defined as follows:

$$\boldsymbol{\varepsilon}_{eq}^{(T)} = \sqrt{T_1^2 + T_{23}^2} \quad \text{where} \quad T_1 = \frac{\sqrt{\boldsymbol{\varepsilon}_{N_1}^2 + \boldsymbol{\varepsilon}_{T_1}^2}}{\chi_1} \quad \text{and} \quad T_{23} = \frac{\sqrt{\boldsymbol{\varepsilon}_{N_{23}}^2 + \boldsymbol{\varepsilon}_{T_{23}}^2}}{\chi_{23}} \tag{23}$$

As can be noted, T_1 and T_{23} are each part of quadratic terms in the failure criterion under tensile loading.

Defining the elastic behavior of the equivalent stress as $\sigma_{eq} = \lambda_4\boldsymbol{\varepsilon}_{eq}$, the exponential softening of the equivalent stress can be expressed as follows:

$$\begin{aligned} \sigma_{eq}^{(T)} &= \lambda_2 \exp\left(-\frac{\left\langle \varepsilon_{eq}^{(T)} - 1 \right\rangle}{\xi_{eq}}\right) \quad \text{for } \varepsilon_{eq}^{(T)} \geq 1 \\ &\text{where } \xi_{eq} = \left(\xi_{23} - \xi_1\right)\left(\xi_{23} - \xi_1\right)^2 - \xi_1 \end{aligned} \tag{24}$$

where $\langle x \rangle = \max(x, 0)$. Transverse and longitudinal tensile strength of UD composite can be achieved by calibrating χ_1 and χ_{23}, respectively. ξ_{eq} governs energy dissipation while the material is under softening. ξ_1 relates to the energy dissipated by mode 1 due to softening, and ξ_{23} relates to the energy dissipated by mode 23. When the longitudinal loading is applied, the value of T_1 is zero, and ξ_{eq} is purely energy dissipated by mode 23. However, T_1 is nonzero when the transverse loading is applied but T_{23} is still dominant. Therefore, ξ_{23} is the dominant parameter in calibrating the energy dissipated in softening under transverse loading. The energy dissipation of UD composite from the softening behavior under the transverse or longitudinal tension can be achieved by calibrating ξ_1 and ξ_{23}.

Once the equivalent stress is computed, normal and shear stress for mode 1, 2 and 3 can be extracted by applying the principle of virtual work. The virtual work done by equivalent stress and strain is expressed as follows:

$$\delta \mathcal{W} = \sigma_{eq} \delta \varepsilon_{eq} = \frac{\sigma_{eq}}{\varepsilon_{eq}} \left(\frac{\varepsilon_N^{(1)} \delta \varepsilon_N^{(1)}}{\chi_1^2} + \frac{\varepsilon_T^{(1)} \delta \varepsilon_T^{(1)}}{\chi_1^2} + \frac{\varepsilon_N^{(23)} \delta \varepsilon_N^{(23)}}{\chi_{23}^2} + \frac{\varepsilon_T^{(23)} \delta \varepsilon_T^{(23)}}{\chi_{23}^2} \right) \tag{25}$$

From Eq. 20, it implies that $\sigma_N^{(1)}$ is proportional to $\frac{\sigma_{eq}}{\varepsilon_{eq}} \frac{\varepsilon_N^{(1)}}{\chi_1^2}$. In order to find the correct proportionality, the virtual work computed from the equivalent stress needs to be thermodynamically consistent. In the elastic regime,

$$\begin{aligned} \delta \mathcal{W} &= \sigma_N^{(1)} \delta \varepsilon_N^{(1)} + \sigma_T^{(1)} \delta \varepsilon_T^{(1)} + \sigma_N^{(23)} \delta \varepsilon_N^{(23)} + \sigma_T^{(23)} \delta \varepsilon_T^{(23)} \\ &= \lambda_1 \varepsilon_N^{(1)} \delta \varepsilon_N^{(1)} + \lambda_1 \varepsilon_T^{(1)} \delta \varepsilon_T^{(1)} + \lambda_2 \varepsilon_N^{(23)} \delta \varepsilon_N^{(23)} + \lambda_2 \varepsilon_T^{(23)} \delta \varepsilon_T^{(23)} \end{aligned} \tag{26}$$

By multiplying proportionality coefficients, each term in Eq. 25 and Eq. 26 can be equated.

$$\alpha_1 \sigma_N^{(1)} = \alpha_1 \lambda_1 \varepsilon_N^{(1)} = \frac{\sigma_{eq}}{\varepsilon_{eq}} \frac{\varepsilon_N^{(1)}}{\chi_1^2} = \frac{\lambda_2}{\chi_1^2} \varepsilon_N^{(1)} \tag{27}$$

$$\alpha_1 = \frac{\lambda_2}{\lambda_1} \frac{1}{\chi_1^2} \tag{28}$$

Then, $\sigma_N^{(1)}$ under softening can be computed,

$$\sigma_N^{(1)} = \frac{\sigma_{eq}}{\varepsilon_{eq}} \frac{\lambda_1}{\lambda_2} \varepsilon_N^{(1)} \tag{29}$$

After the similar process is carried on for other components of stress vectors, it can be shown that:

$$\sigma_T^{(1)} = \frac{\sigma_{eq}}{\varepsilon_{eq}} \frac{\lambda_1}{\lambda_2} \varepsilon_T^{(1)} \qquad \sigma_N^{(23)} = \frac{\sigma_{eq}}{\varepsilon_{eq}} \varepsilon_N^{(23)} \qquad \sigma_T^{(23)} = \frac{\sigma_{eq}}{\varepsilon_{eq}} \varepsilon_T^{(23)} \tag{30}$$

Equivalent strain for the compressive loading is defined as follows:

$$\begin{aligned} \boldsymbol{\varepsilon}_{eq}^{(C)} &= \sqrt{C_1^2 + C_{23}^2} \\ \text{where} \quad C_1 &= \frac{\sqrt{(\beta_1 \varepsilon_{N_1})^2 + \varepsilon_{T_1}^2}}{\gamma_1} \quad C_{23} = \frac{\sqrt{(\beta_{23} \varepsilon_{N_{23}})^2 + \varepsilon_{T_{23}}^2}}{\gamma_{23}} \end{aligned} \tag{31}$$

Similar to the tensile loading, C_1 and C_{23} come from the quadratic terms in the failure criterion under compressive loading.

Defining the elastic behavior of the equivalent stress as $\sigma_{eq} = \lambda_2 \boldsymbol{\varepsilon}_{eq}$, the exponential softening of the equivalent stress can be expressed as follows:

$$\sigma_{eq}^{(C)} = \lambda_2 \exp\left(-\frac{\left\langle \varepsilon_{eq}^{(C)} - 1 \right\rangle}{\eta_{eq}}\right) \quad \text{for } \varepsilon_{eq}^{(C)} \geq 1$$
$$\text{where } \eta_{eq} = (\eta_{23} - \eta_1)(\eta_{23} - \eta_1)^2 - \eta_1 \tag{32}$$

Transverse and longitudinal compressive strength of UD composite can be achieved by calibrating γ_1 and γ_{23}, respectively. η_{eq} governs energy dissipation while the material is under compressive softening. η_1 relates to the energy dissipated by mode 1, and ξ_{23} relates to the energy dissipated by mode 23. When the longitudinal loading is applied, the value of C_1 is zero, and η_{eq} is purely energy dissipated by mode 23. However, C_1 is nonzero when the transverse loading is applied but still C_{23} is dominant. Therefore, η_{23} is the dominant parameter in calibrating the energy dissipated in softening under transverse loading. The energy dissipation of UD composite from the softening behavior under the transverse or longitudinal tension can be achieved by calibrating η_1 and η_{23}.

Once the equivalent stress is computed, the principle of virtual work is applied to obtain the normal and shear stress for mode 1, 2 and 3. The virtual work done by equivalent stress and strain is expressed as follows:

$$\begin{aligned}\delta\mathcal{W} &= \sigma_{eq}\delta\varepsilon_{eq} \\ &= \frac{\sigma_{eq}}{\varepsilon_{eq}}\left(\beta_1^2\frac{\varepsilon_N^{(1)}\delta\varepsilon_N^{(1)}}{\gamma_1^2} + \frac{\varepsilon_T^{(1)}\delta\varepsilon_T^{(1)}}{\gamma_1^2} + \beta_{23}^2\frac{\varepsilon_N^{(23)}\delta\varepsilon_N^{(23)}}{\gamma_{23}^2} + \frac{\varepsilon_T^{(23)}\delta\varepsilon_T^{(23)}}{\gamma_{23}^2}\right)\end{aligned} \tag{33}$$

After applying thermodynamic consistency in the virtual work, it can be shown that, again:

$$\sigma_N^{(1)} = \frac{\sigma_{eq}}{\varepsilon_{eq}}\frac{\lambda_1}{\lambda_2}\varepsilon_N^{(1)} \quad \sigma_T^{(1)} = \frac{\sigma_{eq}}{\varepsilon_{eq}}\frac{\lambda_1}{\lambda_2}\varepsilon_T^{(1)} \quad \sigma_N^{(23)} = \frac{\sigma_{eq}}{\varepsilon_{eq}}\varepsilon_N^{(23)} \quad \sigma_T^{(23)} = \frac{\sigma_{eq}}{\varepsilon_{eq}}\varepsilon_T^{(23)} \tag{34}$$

INELASTIC BEHAVIOR UNDER OUT-OF-PLANE SHEAR LOADING

Mode 4 describes the material deformation when the shear load is applied in the plane of isotropy (plane *1-2*). Out-of-plane shear is an example of this type of shear loading. In the absence of direct experimental data, it is assumed to be stay in elastic regime in this formulation. In practical situations, the effects of this assumption is negligible because out-of-plane shear deformation stays in the elastic regime most of time.

INELASTIC BEHAVIOR UNDER IN-PLANE SHEAR LOADING

Mode 5 describes the material deformation on the in-plane shear loading, and the UD composite of often experiences extensive micro-cracking before the it enters the

inelastic regime. This causes the non-linear elastic behavior in contrast to mode 1, 2 and 3. The expressions for the inelastic behavior of mode 5 are as follow:

$$\sigma_T^{(5)} = \left(s^{(5)}\right)^{1-p} \left(\lambda^{(5)}\right)^p \begin{cases} \left(\varepsilon^{(5-t)}\right)^p, & \text{if } \varepsilon^{(5-t)} \leq s^{(5)}/\lambda^{(5)} \\ \left(k_{at}^{(5)}\right)^p \left\langle 1 - \frac{\left\langle \varepsilon^{(5-t)} - k_{at}^{(5)} \right\rangle}{k_{bt}^{(5)}} \right\rangle, & \text{if } \varepsilon^{(5-t)} > s^{(5)}/\lambda^{(5)} \end{cases} \tag{35}$$

for $\varepsilon_N^{(5)} \geq 0$ and

$$\sigma_C^{(5)} = \left(c^{(5)}\right)^{1-p} \left(\lambda^{(5)}\right)^p \begin{cases} \left(\varepsilon^{(5-c)}\right)^p, & \text{if } \varepsilon^{(5-c)} \leq c^{(5)}/\lambda^{(5)} \\ \left(k_{ac}^{(5)}\right)^p \left\langle 1 - \frac{\left\langle \varepsilon^{(5-c)} - k_{ac}^{(5)} \right\rangle}{k_{bc}^{(5)}} \right\rangle, & \text{if } \varepsilon^{(5-c)} > s^{(5)}/\lambda^{(5)} \end{cases} \tag{36}$$

for $\varepsilon_N^{(5)} < 0$. The functions $s^{(5)}(\theta, \varphi) = s_0^{(5)}$ and $c^{(5)}(\theta, \varphi) = c_0^{(5)}$ are assumed to be uniform for all the microplanes, and indicate the tensile and compressive linear elastic limits in mode 5. Material will be subjected to the nonlinear behavour over these stresses. p is the order of the nonlinearity and assumed to be same for both tension and compression. The parameters $k_{at}^{(5)}$ and $k_{ac}^{(5)}$ refers to the value of the effective strain that initiate the linear softening whereas the parameters $k_{bt}^{(5)}$ and $k_{bc}^{(5)}$ are defined such that $\sigma^{(5)} = 0$ when the effective strain is reached $k_{bt}^{(5)} + k_{at}^{(5)}$ or $k_{bc}^{(5)} + k_{ac}^{(5)}$ in tension or compression, respectively.

CALIBRATION AND VALIDATION

Thanks to the collection of data in the "World Wide Failure Exercise [15]," all the calibration performed in this study is validated by comparing the numerical simulation to the experimental data. First, uniaxial test was performed with a single element of the size of $1mm \times 1mm \times 1mm$ that represents 0° laminae to obtain the correct stiffness value and uniaxial strength.

Material choice

The unidirectional composite material used for the calibration and validation has Silenka E-Glass 1200tex fibers, and MY750/HY917/DY063 epoxy was used for matrix. Manufacturer of this material is DLR. According to the "World Wide Failure Exercise [15]," Filament winding technology was used in preparing the test specimens. Mechanical properties of the unidirectional laminae provided in the "World Wide Failure Exercise [15]," are listed in Table I.

TABLE I. MECHANICAL PROPERTIES OF THE SELECTED UD COMPOSITE

Fiber Type Matrix Type		Silenka E-Glass 1200tex MY750/HY917/DY063
Longitudinal modulus: E_1	[MPa]	45600
Transverse modulus: E_2	[MPa]	16200
In-plane shear modulus: G_{12}	[MPa]	5830
Major Poisson's ratio: ν_{12}	-	0.278
Through thickness Poisson's ratio: ν_{23}	-	0.4
Longitudinal tensile strength	[MPa]	1280
Longitudinal compressive strength	[MPa]	800
Transverse tensile strength	[MPa]	40
Transverse compressive strength	[MPa]	145
In-plane shear strength	[MPa]	73
Longitudinal tensile failure strain	%	2.807
Longitudinal compressive failure strain	%	1.754
Transverse tensile failure strain	%	0.246
Transverse compressive failure strain	%	1.2
In-plane shear failure strain	%	4

Uniaxial calibration

The stress-strain curves for the tensile/compressive loading is presented in Figure 2. As can be noted, the elastic strengths provided by the microplane model have a good agreement with the experimental data. However, the fracture energy of the material, which is neccesary to calibrate the post-peak softening behavior, was not available. Therefore, fracture energies for longitudinal tension, longitudinal compression, transverse tension, transverse compression, and in-plane shear loading were roughly estimated as: 150, 170, 0.8, 6.0, and 7.5 N/mm, respectively.

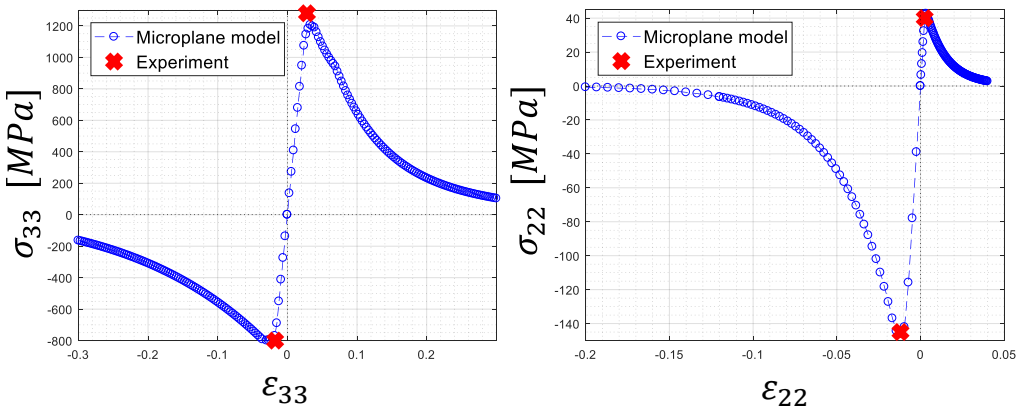

Figure 2. Stress-strain relationship for tensile/compressive loading condion

The full set of calibration parameters for the E-glass UD composite is shown in Table II.

TABLE II. CALIBRATION VALUES FOR THE SELECTED MATERIAL

Calibration parameter		
Mode 1 tensile strength: $\lambda_1\chi_1$	[MPa]	20.0
Mode 1 compressive strength: $\lambda_1\gamma_1$	[MPa]	55.0
Shear dominant failure angle: β_1	-	0.4
Mode 1 tensile energy density ξ_1	[MPa]	4.0
Mode 1 compressive energy densityη_1	[MPa]	3.0
Mode 23 tensile strength: $\lambda_2\chi_{23}$	[MPa]	1020.0
Mode 23 compressive strength: $\lambda_2\gamma_{23}$	[MPa]	500.0
Fiber misalignment factor: β_{23}	-	0.7
Mode 23 tensile energy density: ξ_{23}	[MPa]	2.0
Mode 23 compressive energy density: η_{23}	[MPa]	10.0
Degree of nonlinearity in Shear mode: p	-	0.3
Mode 5 tensile linear-elastic limit: $s^{(5)}$	[MPa]	29
Mode 5 tensile nonlinearity limit: $k_{at}^{(5)}$	-	0.038
Mode 5 tensile-failure strain: $k_{bt}^{(5)}$	-	0.015
Mode 5 compressive linear-elastic limit: $c^{(5)}$	[MPa]	29
Mode 5 compressive nonlinearity limit: $k_{ac}^{(5)}$	-	0.038
Mode 5 compressive-failure strain: $k_{bc}^{(5)}$	-	0.015

CONCLUSION

This contribution proposes a theoretical framework to simulate the orthotropic stiffness, pre-peak nonlinearity, failure envelopes, and the post-peak softening and fracture of unidirectional composites. The microplane formulation with constitutive laws defined on planes of several orientations within the mesostructure allows a sound and physically-based description of the damage mechanisms occurring in UD composites whereas the spectral decomposition of the microplane strains and stresses provides a rigorous generalization of the formulation to anisotropy. Each eigenmode can be easily associated to the mechanical behavior of a particular constituent at the mesostructure and to a particular type of deformation. This makes it easy to take advantage of each eigenmode to define constitutive laws at microplane level targeting different damaging and fracturing mechanisms; Applied to a glass UD composite, the model showed a good agreement with uniaxial tests in tension and compression for various lay-ups. In particular, the model captured the highly non-linear mechanical behavior under off-axis and shear loading, which is typical of composites and is characterized by diffuse subcritical microcracking of the polymer matrix. This feature is of utmost importance in all situations in which predicting energy absorption is key, such as in crashworthiness analyses. Currently, the model is under the validation of multiaxial behavior of UD composites. Biaxial envelop of the E-glass composite will be constructed and compared with the experimental data in "World Wide Failure Exercise [15]."

Different from strength-based criteria abundant in the literature, the formulation is endowed with a characteristic length through coupling with the crack band model.

This ensures objective numerical analysis of softening damage and prevents spurious mesh sensitivity. Further, this is key to capture the intra-laminar size effect, a salient feature of composite structures. This aspect, often overlooked in the literature on composites, is a determinant factor for damage tolerance design of large composite structures. The model is computationally efficient and capable of analysing the fracturing behavior of large composite structures, making it a valuable design tool for e.g. crashworthiness applications.

REFERENCES

1. Cusatis, G., Beghini, A., and Bažant, Z.P., 2008. "Spectral Stiffness Microplane Model for Quasibrittle Composite Laminates – Part I: Theory," Journal of Applied Mechanics, 75(2): 021009.

2. Beghini, A., Cusatis, G., and Bažant, Z.P., 2008. "Spectral Stiffness Microplane Model for Quasibrittle Composite Laminates – Part II: Calibration and Validation," Journal of Applied Mechanics, 75(2): 021010.

3. Salviato, M., Ashari, S. and Cusatis, G., 2016. "Spectral Stiffness Microplane Model for Damage and Fracture of Textile Composites," Composite Structures, 137: 170-184.

4. Kirane, K., Salviato, M., and Bažant, Z.P., 2016. "Microplane triad model for simple and accurate prediction of orthotropic elastic constants of woven fabric composites," Journal of Composite Materials, 50(9): 1247-1260.

5. Kirane, K., Salviato, M., and Bažant, Z.P., 2016. "Microplane-Triad Model for Elastic and Fracturing Behavior of Woven Composites," Journal of Applied Mechanics. 83(4): 041006.

6. Jin, C., Salviato, M., Li, W., and Cusatis, G., 2017. "Elastic microplane formulation for transversely isotropic materials," Journal of Applied Mechanics, 84(1): 011001.

7. Li, W., Salviato, M., and Cusatis, G., 2017. "Spectral Stiffness Microplane Modeling of Fracture and Damage of 3D Woven Composites," In Proceedings of the American Society for CompositesThirty-second Technical Conference.

8. Caner, F.C., and Bažant, Z.P., 2012"Microplane model M7 for plain concrete. II: Calibration and verification," Journal of Engineering Mechanics, 139(12): 1724-1735.

9. Bažant, Z.P., Caner, F.C., Carol, I., Adley, M.D., and Akers, S.A., 2000. "Microplane model M4 for concrete. I: Formulation with work-conjugate deviatoric stress." Journal of Engineering Mechanics, 126(9): 944-953.

10. Theocaris, P.S., and Sokolis, D.P., 1998. "Spectral decomposition of the compliance tensor for anisotropic plates," Journal of Elasticity, 51(2): 89-103.

11. Theocaris, P.S., and Sokolis, D.P., 1999. "Spectral decomposition of the linear elastic tensor for monoclinic symmetry," Acta Crystallogr Sect A: Found Crystallogr, 55: 635-647.

12. Theocaris, P.S., and Sokolis, D.P., 2000. “Spectral decomposition of the compliance fourth rank tensor for orthotropic materials,” Archive of Applied Mechanics, 70(4): 289-306.

13. Cusatis, G., Pelessone D., and Mencarelli A., 2011. “Lattice discrete particle model (LDPM) for failure behavior of concrete. I: theory, Cement and Concrete Composites,” 33(9): 881-890.

14. Cusatis G., Bažant Z.P., and Cedolin L., 2003. “Confinement-Shear Lattice Model for Concrete Damage in Tension and Compression: I. Theory,” Journal of Engineering Mechanics ASCE, 129(12): 1439-1448.

15. Soden, P.D., Hinton, M.J., and Kaddour, A.S., “Lamina properties, lay-up configurations and loading conditions for a range of fibre reinforced composite laminates,” Failure Criteria in Fibre Reinforced Polymer Composites, The World-Wide Failure Exercise, Ch. 2.1, Elsevier Ltd, 2004, pp. 30-51.